A Raman Spectroscopic Characterization of Bonding in the Complex of Horse Liver Alcohol Dehydrogenase with NADH and *N*-Cyclohexylformamide†

Hua Deng,*,‡ John F. Schindler,§ Kristine B. Berst,§ Bryce V. Plapp,§ and Robert Callender‡

Department of Biochemistry, Albert Einstein College of Medicine, Bronx, New York 10461, and Department of Biochemistry, The University of Iowa, Iowa City, Iowa 52242

Received June 22, 1998

ABSTRACT: The binding of *N*-cyclohexylformamide (CXF) to the complex of horse liver alcohol dehydrogenase with NADH mimics that of the Michaelis complex for aldehyde reduction catalyzed by the enzyme. The Raman spectra of bound CXF and its ^{13}C- and ^{15}N-substituted derivatives have been obtained using Raman difference techniques, and the results are compared with CXF spectra in aqueous solution and in methylene chloride. The results indicate that the amide N−H bond is trans to the C═O bond of CXF both in solution and in the enzyme ternary complex. The C═O stretch and N−H bending modes of the amide of CXF shift −16 and −9 cm^{-1}, respectively, in the enzyme ternary complex relative to that in aqueous solution and −48 and 36 cm^{-1}, respectively, relative to that in methylene chloride. Ab initio normal mode calculations on various model systems of CXF show that the observed frequency changes of the C═O stretch mode have contributions from the frequency changes induced by the environmental changes near both the local C═O bond and the remote N−H bond. The same is true for the observed N−H bending frequency change. Our calculations also show that the environmentally induced frequency changes are additive so that it is possible to determine the C═O stretch (or N−H bending) frequency change that is due to the local interaction change near the C═O (or N−H) bond from the observed frequency changes. On the basis of these results and the empirical relationship between the C═O stretch frequency shift and the interaction enthalpy change on the C═O bond developed here, it is found that the C═O group of CXF in the enzyme/NADH/CXF complex binds with a favorable interaction enthalpy of approximately 5.5 kcal/mol relative to water. Similar analysis suggests that the N−H moiety of CXF is destabilized in the ternary complex by about 1.5 kcal/mol relative to water but is stabilized by about 1.5 kcal/mol relative to a hydrophobic environment. The analysis describes quantitatively the binding of the C═O of CXF with the catalytic zinc and the hydroxyl group of Ser-48 and the interaction of the N−H with the benzene ring of Phe-93 of the enzyme.

Horse liver alcohol dehydrogenase [EC 1.1.1.1 (LADH[1])] catalyzes the reactions of aldehydes and their corresponding alcohols with the coenzymes NADH and NAD$^+$. *N*-Cyclohexylformamide (CXF) is an analogue of an aldehyde substrate as it is an uncompetitive inhibitor of LADH against varied concentrations of ethanol and a competitive inhibitor against acetaldehyde. It binds to the enzyme/NADH complex with an apparent inhibition constant of 8 μM (*1*). Amides, like CXF, inhibit alcohol metabolism and might be useful therapeutic agents, for example in preventing the oxidation of methanol or ethylene glycol to their toxic acids (*2*, *3*). A structure of LADH complexed with NADH and CXF determined by X-ray crystallography at 2.5 Å resolution shows that the carbonyl oxygen of the formamide coordinates to the catalytic zinc ion and forms a hydrogen bond with the hydroxyl group of Ser-48 (*1*). Moreover, the carbonyl carbon is positioned appropriately for direct transfer of a hydride ion from the NADH. Thus, the complex apparently mimics the Michaelis complex of NADH and aldehyde.

In this study, Raman difference spectroscopic techniques are used to determine the vibrational spectrum of CXF bound to the LADH/NADH complex and for CXF in water and in a hydrophobic solvent. The aim of this study is to characterize the interactions between the amide of CXF when it is bound to the LADH/NADH complex, and thus to reveal how the enzyme affects the ground state structure of the reactants. A detailed picture of binding is obtained by monitoring the vibrational spectrum of the bound ligand, and when the vibrational results are combined with the crystallographic picture of the ternary complex, a detailed picture of how the protein accomplishes ligand binding emerges. Significant frequency changes are observed for the amide C═O stretch, the C−N stretch, and the N−H bending frequencies for bound CXF compared to their solution counterparts. The frequency shifts arise from changes in hydrogen bonding and other electrostatic interactions with the C═O and N−H bonds upon binding. To interpret the vibrational results, a normal-mode analysis, based on ab initio calculations, is performed. Furthermore, empirical correlations that quantitatively relate the shifts in frequency to

† This work was supported by NIH Grants GM35183 (R.C.) and AA00279 (B.V.P.).

‡ Albert Einstein College of Medicine.

§ The University of Iowa.

[1] Abbreviations: LADH, horse liver alcohol dehydrogenase; CXF, *N*-cyclohexylformamide.

S0006-2960(98)01477-9 CCC: $15.00
Published on Web 09/18/1998

effective local changes in hydrogen bond strength and/or electrostatic interaction are developed. The conclusions derived from the normal-mode analysis, as well as the empirical correlations that are developed here for the amide of CXF, can also be applied to the structurally sensitive amide of the peptide linkage and other amide systems. Hence, they should be very useful in interpreting vibrational structural studies of proteins that are based on measurements of the amide bands in proteins.

MATERIALS AND METHODS

Materials. Crystalline horse liver ADH (EE isoenzyme), NAD^+, and NADH were purchased from Boehringer Mannheim. Sodium [^{13}C]formate (99%), [^{15}N]ammonium acetate (98%), methyl orthoformate, *p*-toluenesulfonic acid, cyclohexylamine, and sodium methoxide were purchased from Aldrich and were used without further purification. $H_2{}^{18}O$ (0.6% ^{16}O, 4.8% ^{17}O, and 94.6% ^{18}O) was purchased from Isotech Inc. *N*-Cyclohexylformamide from Aldrich was purified using a silica gel column developed with ethyl acetate/hexane (60/40).

The labeled *N*-cyclohexylformamides were prepared by the general procedure developed previously (*4*).

N-[formyl-^{13}C]Cyclohexylformamide. Sodium [^{13}C]formate (1.0 g) was added to 3 mL of water, followed by the addition of 1.38 mL of concentrated HCl and 3.23 mL of cyclohexylamine. The reaction mixture was refluxed while being stirred for 1 h, and the solvent was removed under reduced pressure. Toluene (10 mL) was added to the residue, and the reaction mixture was allowed to reflux for 1 h. The toluene/H_2O azeotrope was removed by distillation at 88 °C. Reflux and distillation were repeated twice. The excess toluene was removed under reduced pressure, and the remaining residue was dissolved in $CHCl_3$. The organic layer was washed with water, dried with $MgSO_4$, and filtered. The solvent was removed under reduced pressure, and the residual oil was applied to a silica gel column and eluted with ethyl acetate/hexane (60/40). The product was isolated as a colorless oil and was not dried. ^{1}H NMR ($CDCl_3$): δ 1.05−1.45 (m, 5H, CH_2), 1.56−2.02 (m, 5H, CH_2), 3.20−3.43 (m, 0.3H, ring-CH), 3.77−3.99 (m, 0.7H, ring-CH), 5.37−5.79 (d, broad, NH), 8.08 (dd, 0.7H, CHO, $^1J_{CH}$ = 191 Hz, $^3J_{CH-NH} \leq 1$ Hz), 8.10 (dd, CHO, 0.3H, $^1J_{CH}$ = 188 Hz, $^3J_{CH-NH}$ = 12.0 Hz). The coupling constants indicate that 70% of the compound has the N−H trans to the C═O. EIMS: *m*/*z* 128 (M^+).

N-[^{15}N]Cyclohexylformamide. [^{15}N]Cyclohexylamine was synthesized by the procedure of Borch et al. (*5*) and then converted to the formamide as described above. ^{1}H NMR ($CDCl_3$): δ 1.05−1.47 (m, 5H, CH_2), 1.56−1.81 (m, 5H, CH_2), 3.39−3.77 (m, 0.3H, ring-CH), 3.77−3.94 (m, 0.7H, ring-CH), 5.50 (ddd, 0.7H, NH, $^1J_{NH}$ = 89 Hz, $^3J_{NH-CH}$ = 8.5 Hz, $^3J_{NH-CHO}$ = 1.6 Hz), 6.01 (ddd, 0.3H, NH, $^1J_{NH}$ = 87 Hz, $^3J_{NH-CH}$ = 10.3 Hz, $^3J_{NH-CHO}$ = 1.8 Hz), 8.086 (ddd, 0.7H, CHO, $^2J_{CH-N}$ = 14.9 Hz, $^3J_{CH-NH}$ = 1.9 Hz, $^4J_{CH-CH}$ = 0.93 Hz), 8.092 (ddd, 0.7H, CHO, $^2J_{CH-N}$ = 14.3 Hz, $^3J_{CH-NH}$ = 10.5 Hz, $^4J_{CH-CH}$ = 0.53 Hz). EIMS: *m*/*z* 128 (M^+).

N-[^{18}O]Cyclohexylformamide. Sodium [^{18}O]formate was synthesized by a modified procedure of Risley and Van Etten (*6*). To 5.4 mmol of methylorthoformate was added 0.2 mL of $H_2{}^{18}O$ followed by the addition of 50 mg of *p*-toluenesulfonic acid. The reaction mixture was stirred for 5 min, and 10 mL of 0.5 M sodium methoxide was added followed by 0.2 mL of $H_2{}^{18}O$. The solvent was removed under reduced pressure, and the sodium [^{18}O]formate was washed with dry THF. The sodium [^{18}O]formate was collected by filtration and converted to *N*-cyclohexylformamide by the procedure described above. ^{1}H NMR ($CDCl_3$): δ 1.11−1.43 (m, 5H, CH_2), 1.58−1.68 (m, 1H, CH_2), 1.68−1.80 (m, 2H, CH_2), 1.86−1.98 (m, 2H, CH_2), 3.26−3.38 (m, 0.3H, CH), 3.81−3.94 (m, 0.7H, CH), 5.29−5.69 (d, broad, 1H, NH), 8.11 (d, 0.7H, CHO, $^3J_{CH-NH} \leq 1$ Hz), 8.13 (d, 0.3H, CHO, $^3J_{CH-NH}$ = 12.5 Hz). EIMS: *m*/*z* 129 and 127 (M^+) in equal intensities.

The exchangeable hydrogen of *N*-cyclohexylformamide was replaced with deuterium by dissolving 5−10 mg of *N*-cyclohexylformamide in 1 mL of D_2O, stirring overnight, and removing excess D_2O under reduced pressure.

The samples of LADH for Raman spectra were prepared by dialysis of LADH with 100 mM sodium pyrophosphate hydrochloride buffer at pH 9.6 or with 66 mM sodium phosphate and 100 mM KCl buffer at pH 8. After dialysis, the enzyme was concentrated by ultrafiltration with a Centricon30 apparatus (Amicon). Concentrations of LADH and NADH were determined spectroscopically using an ϵ_{280} of 3.57×10^4 M^{-1} cm^{-1} for LADH and an ϵ_{340} of 6.22×10^3 M^{-1} cm^{-1} for NADH. Typically, the ternary complex of LADH/NADH/CXF was prepared in a 1.5/2.5/2.5 molar ratio. Under these conditions, all of the *N*-cyclohexylformamide was enzyme-bound. All samples were maintained at 4 °C.

Spectroscopy. NMR spectra were determined with a Varian 500 MHz NMR spectrometer and mass spectra with a Trio-1 spectrometer from VG Analytical (Manchester, England) with separation on a J&W Scientific DBI GC column (0.32 μm × 15 m).

The Raman spectra were measured using an optical multichannel analyzer system. This system uses a Triplemate spectrometer (Spex Industries, Metuchen, NJ) with a model DIDA-1000 reticon detector connected to an ST-100 detector (Princeton Instruments, Trenton, NJ). The 514.5 nm line from an argon ion laser was used to irradiate the sample (∼100 mW). Separate spectra for enzyme and enzyme/inhibitor complexes in solution (approximate concentration of 1.5 mM) were measured using a special split cell (the volume of each side being about 30 μL) and a sample holder with a linear translator as previously described (*7*). The spectrum in one side of the split cuvette was taken; the split cell was translated, and the spectrum in the other side was taken. This sequence was repeated until sufficient signal to noise was obtained. A difference spectrum was generated by numerically subtracting the sum of the spectra obtained from each side. In general, the two summed spectra do not subtract to zero, as judged by the subtraction of well-known protein marker bands (for example, the amide I, amide III, and the 1450 cm^{-1} bands, the latter band being especially useful since it is generally not affected by protein conformational changes). These protein marker bands are determined from their bandwidths (generally much broader than those from spectra of bound substrates) and their characteristic positions. Hence, one summed spectrum is scaled by a small numerical factor, generally between 1.05 and 0.95,

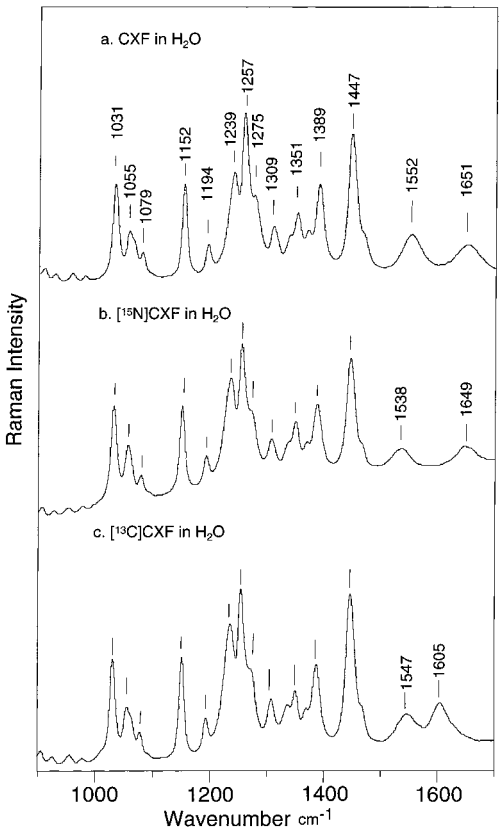

FIGURE 1: Raman spectra of *N*-cyclohexylformamide (CXF) in H_2O (200 mM) at 4 °C: (a) unlabeled CXF, (b) [^{15}N]CXF, and (c) [^{13}C]-CXF. The Raman bands that shift by less than 2 cm^{-1} in the ^{13}C- or ^{15}N-substituted CXF spectra relative to those in panel a are marked but not labeled.

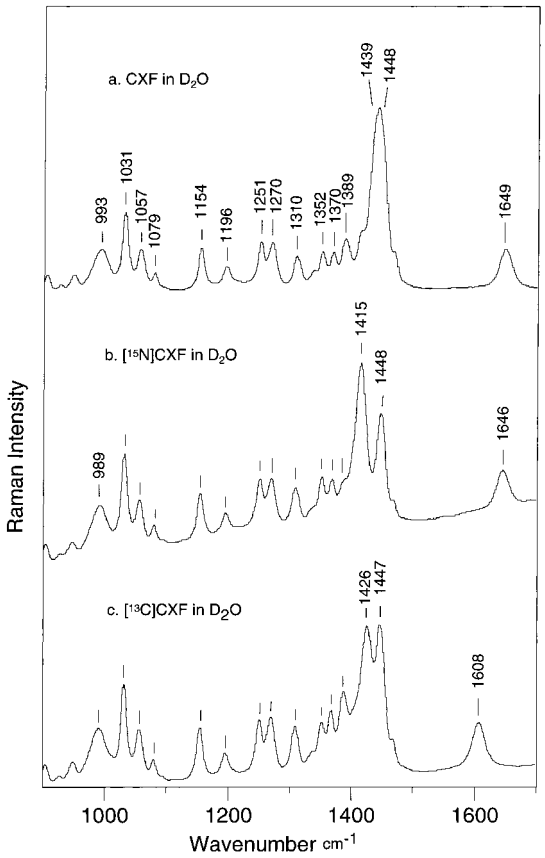

FIGURE 2: Raman spectra of *N*-cyclohexylformamide (CXF) in D_2O (200 mM) at 4 °C: (a) unlabeled CXF, (b) [^{15}N]CXF, and (c) [^{13}C]-CXF. The Raman bands that shift by less than 2 cm^{-1} in the ^{13}C- or ^{15}N-substituted CXF spectra relative to those in panel a are marked but not labeled.

which is adjusted until the protein bands are nullified. This procedure is demonstrated in the Appendix. A spectral calibration is carried out for each measurement using the known Raman lines of toluene, and absolute band positions are accurate to within ±2 cm^{-1}. None of the spectra presented here have been smoothed.

Computational Analysis. The ab initio Hartree−Fock method (using the 6-31G** basis set), as implemented in Gaussian 94 (*8*), was used to optimize the geometry of the model compounds of *N*-cyclohexylformamide complexed with water molecule(s) and/or a Na^+ ion. The vibrational normal modes were then calculated on these geometrically optimized model compounds using the same basis set.

RESULTS

Raman Spectra of N-Cyclohexylformamide. The Raman spectra of CXF and its ^{15}N and ^{13}C amide-substituted derivatives in H_2O and D_2O are given in Figures 1 and 2. Previous studies on various N-monosubstituted amides have shown that vibrational spectroscopy can be used to distinguish two geometries of the amides: those with the N−H and C═O bonds in the cis configuration and those with these two bonds in the trans configuration (cf. refs *9* and *10* and references therein). In the cis isomer, the in-plane N−H bending mode is around 1450 cm^{-1} and the C−N stretch mode is around 1330 cm^{-1}. The N−H bending is not coupled with the C−N stretch in this geometry so that the C−N stretch mode is affected little when the amide is deuterated. In contrast, the N−H bending and the C−N stretch motions are strongly coupled in the trans geometry to form one mode around 1540 cm^{-1} (sometimes called the amide II or N−H bending mode) and another mode around 1280 cm^{-1} (sometimes called amide III or C−N stretch), respectively (cf. refs *11* and *12*). Because of the coupling, deuteration of the amide results in large frequency shifts for both of these two modes. In Figure 1a, the 1552 cm^{-1} band shifts down by 14 cm^{-1} to 1538 cm^{-1} in the ^{15}N-substituted derivative (Figure 1b); it disappears altogether from this region when the nitrogen is deuterated (Figure 2a). Hence, it is related to the N−H bending motion. Since this band also shifts down by 5 cm^{-1} to 1547 cm^{-1} in the ^{13}C-labeled derivative (Figure 1c), we conclude that this mode also contains some C−N stretch motion. Thus, this mode can be assigned to the amide II mode. Moreover, the geometry of the amide moiety of CXF in aqueous solution is determined to be trans (see above).

The 1239 cm^{-1} band (Figure 1a) disappears upon deuteration of the sample (Figure 2a) but is not sensitive to ^{13}C (Figure 1c) or ^{15}N substitutions (Figure 1b). The normal mode calculations suggest that this mode contains significant contributions from the amide N−H (in plane) bend and several C−H bending motions within the ring. Thus, it is not the expected "normal" amide III mode, although amide III modes are often complex and mix with side chain motions (*11*). The band at 1389 cm^{-1} band shifts down by 10 cm^{-1} upon ^{18}O labeling of the C═O moiety (data not shown); thus, it can be assigned to the H−C═O bending mode. The band at 1651 cm^{-1} in Figure 1a shifts down to 1605 cm^{-1} with

^{13}C (Figure 1c), suggesting that this mode is the C═O stretch mode (amide I mode). The 46 cm^{-1} shift of this mode is larger than the 37 cm^{-1} shift expected for an isolated diatomic C═O stretch. Thus, the C═O stretch motion must be coupled with other atomic motions of the CXF; this will be verified in normal mode calculations reported later in this paper. The rest of the bands in Figure 1a shift less than 2 cm^{-1} in ^{13}C- or ^{15}N-substituted derivatives (Figure 1b,c) and so are related to motions of the cyclohexyl ring.

Throughout this study, the amide I like mode will be referred to as the C═O stretch and the amide II like mode as the N−H bend.

A new band with unusually strong intensity appears at 1439 cm^{-1} in the Raman spectrum of CXF suspended in D_2O (Figure 2a). We can assign this mode to the amide C−N stretch on the basis of its 24 cm^{-1} shift in [^{15}N]CXF (Figure 2b) and 13 cm^{-1} shift in [^{13}C]CXF (Figure 2c). This mode is absent in the Raman spectrum of CXF in H_2O because the C−N stretch and the N−H bending motions are strongly coupled in the trans isomer, as mentioned above. Upon deuterium exchange of the amide hydrogen, the extent of this coupling is greatly diminished due to the much lower N−D bending frequency. The new band at 993 cm^{-1} in the Raman spectrum of CXF in D_2O is most likely the (now isolated) N−D bending mode. The shifts of this band upon ^{15}N and ^{13}C substitution are only 4 and 2 cm^{-1}, respectively, showing that the N−D bending motion is largely decoupled from the C−N stretch motion and contains little contribution from the motion of the amide nitrogen. The ^{13}C substitution-induced shift of the C═O stretch mode in deuterated CXF at 1649 cm^{-1} is reduced to 41 cm^{-1} (Figure 2), closer to that expected for a simple diatomic oscillator, suggesting that the C═O stretch motion is less coupled with other motions of CXF compared with that of the protonated CXF. Thus, in subsequent studies of CXF complexed with LADH, deuterated samples were used to access environmental changes near C═O bond upon binding more accurately. On the other hand, the N−H bending mode can be positively identified by ^{15}N labeling while the N−D bending mode cannot; hence, protonated protein complexes were used to characterize environmental changes of the N−H bond on the basis of N−H bending frequency changes.

The Raman band intensities of enzyme-bound CXF are very weak so that the difference spectrum between LADH/NADH/CXF and LADH/NADH is dominated by the bands that arise from the apoprotein and NADH when CXF binds to the binary complex (see the Appendix). Therefore, it is necessary to employ isotope editing techniques (*13*); the difference Raman spectrum is obtained between complexes of LADH/NADH with unlabeled and isotopically substituted amide. One disadvantage of such experiments is that band positions will appear to be shifted from their true positions when the isotopic shift of a vibrational mode is smaller than its Raman bandwidth. However, it has been shown that, assuming that the band intensities and bandwidths of a vibrational mode do not change upon isotope substitution, the frequency shift of a particular mode for a molecule in two different environments can be calculated with high precision using either the shift of the zero crossing points of the positive/negative doublet observed in the isotope-edited spectrum or the difference in the average frequencies of the negative/positive peaks (*13*, *14*).

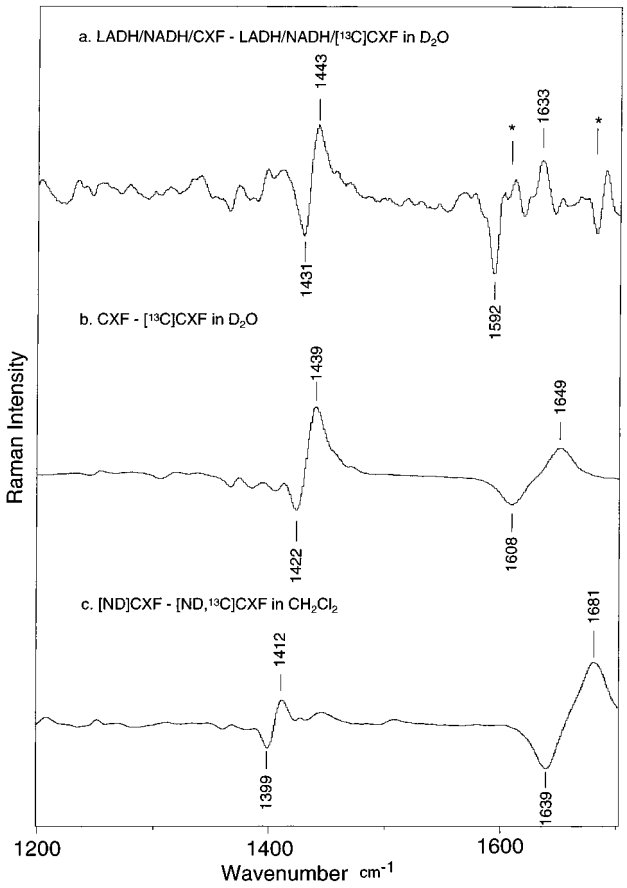

FIGURE 3: Raman difference spectra between unlabeled CXF and [^{13}C]CXF. (a) Between LADH/NADH/*N*-cyclohexylformamide (CXF) and LADH/NADH/[^{13}C]CXF at 4 °C in 100 mM pyrophosphate buffer at pH 9.6 (pH meter reading) in D_2O. The Raman bands marked with an asterisk are due to bound NADH. (b) Between CXF and [^{13}C]CXF at 4 °C in D_2O. (c) Between CXF and [ND,^{13}C]CXF (deuterated amide) at 4 °C in methylene chloride.

Figure 3a shows the difference spectrum between the LADH/NADH/CXF ternary complex and the ternary complex formed with the [^{13}C]CXF prepared in D_2O. For comparison, Figure 3b shows the difference Raman spectrum between CXF and [^{13}C]CXF in D_2O, and Figure 3c shows the difference Raman spectrum between nitrogen-deuterated [ND]CXF and [ND,^{13}C]CXF in methylene chloride. It can be seen that the spectral region between 1500 and 1700 cm^{-1} in Figure 3a is quite crowded. There are more Raman bands in this region than just the anticipated positive−negative C═O stretch mode of CXF. Additional experiments, described in detail in the Appendix, indicate that the positive/negative pair at 1633/1592 cm^{-1} in Figure 3a is the C═O stretch mode. The 1633 cm^{-1} band only appears in the difference spectrum between LADH/NADH/CXF and LADH (Figure 8d in the Appendix), while the 1592 cm^{-1} band (as a shoulder) only appears in the difference spectrum between LADH/NADH/[^{13}C]CXF and LADH (Figure 8e in the Appendix). The control experiments also show that those features in Figure 3a marked with an asterisk are due to NADH. These features appear in the isotope-edited difference spectrum of Figure 3a because (a) the binding of the CXF to LADH/NADH causes a small shift and/or intensity changes of the NADH bands at 1598, 1615, and 1682 cm^{-1} (cf. Figure 8d in the Appendix) and (b) there is inevitably a small mismatch of the unlabeled and ^{13}C-substituted CXF

concentrations in their respective ternary complexes. Hence, these NADH bands are not nullified completely in the isotope-edited spectrum.

The C═O bond of bound CXF is polarized compared to CXF in water, which results in a frequency downshift of the C═O stretch relative to its position in aqueous solution (downshifted by 16 cm^{-1}), and even more so compared to that in methylene chloride (C═O stretch downshifted by 48 cm^{-1}). Such a shift of the C═O stretch frequency is consistent with expectations of stronger hydrogen bonding to the C═O bond of the bound inhibitor relative to aqueous environments which is, in turn, reduced or eliminated when the C═O bond is transferred to methylene chloride (see below). Another positive/negative feature at 1443/1431 cm^{-1} in Figure 3a is assigned to the C−N stretch mode of the CXF. A similar feature was also observed in the difference spectrum between ternary complexes formed with ^{15}N-substituted and unlabeled CXF (data not shown), supporting this assignment. This mode shifts up by 7 cm^{-1} in D_2O (Figure 3b, average frequencies are used) and 32 cm^{-1} in methylene chloride (Figure 3c), both shifts relative to the values for the enzyme-bound CXF. As discussed below, these shifts are also consistent with a stronger hydrogen bonding to and/or electrostatic interaction with the C═O bond of the bound inhibitor compared to those in the other environments.

The difference spectrum between the LADH/NADH/CXF ternary complex and LADH/NADH/[^{15}N]CXF in H_2O is shown in Figure 4a. For comparison, panels b and c of Figure 4 show the analogous difference Raman spectra for CXF in H_2O and in methylene chloride, respectively. Since the ^{15}N isotopic shift of the N−H bending mode is relatively small, the positive/negative feature related to the N−H bending motion at 1543/1524 cm^{-1} in Figure 4a is very weak; its peak−peak intensity is only 0.8% of that of the protein amide I band. Nevertheless, on the basis of the frequency of this mode, as well as the appearance of the new peak at 1443/1431 cm^{-1} in the deuterated complex (Figure 3a), it can be concluded that this is the amide II mode of CXF. Thus, the N−H moiety remains trans to C═O when CXF is bound to the LADH/NADH complex as judged from the response of the mode to labeling (see above), consistent with the X-ray results (*1*). Another derivative feature at 1236/1227 cm^{-1} is related to the C1−N−C stretch motion as shown by normal mode calculations. By comparing panels b and c of Figure 4, we can see that, when CXF is transferred from aqueous solution to methylene chloride, its N−H bending mode shifts down by an average of 43 cm^{-1}. Furthermore, its Raman intensity is substantially reduced relative to the C═O stretch band intensity, from an intensity ratio of 1/1 in aqueous solution (Figure 1) to about 1/5 in methylene chloride. The shift of the N−H bending frequency of the CXF in the LADH ternary complex is −8 cm^{-1} from its value in aqueous solution and is 35 cm^{-1} relative to that in methylene chloride (Figure 4, using the average frequencies of the peaks in the positive/negative features to calculate the shifts). Thus, it would appear that the hydrogen bonding strength of the N−H bond of CXF in the ternary complex, which is expected to be reflected in shifts of the N−H bend, is similar to that in aqueous solution but quite different from that in methylene chloride. However, since the amide moiety is highly conjugated, the N−H bending frequency of CXF may also be affected by the changes of the C═O bond stretch frequency, and vice versa. To investigate such a possibility, so we are able to estimate quantitatively hydrogen bond interaction energies between protein and the C═O and the N−H moieties in the ternary complex, ab initio normal mode calculations were performed.

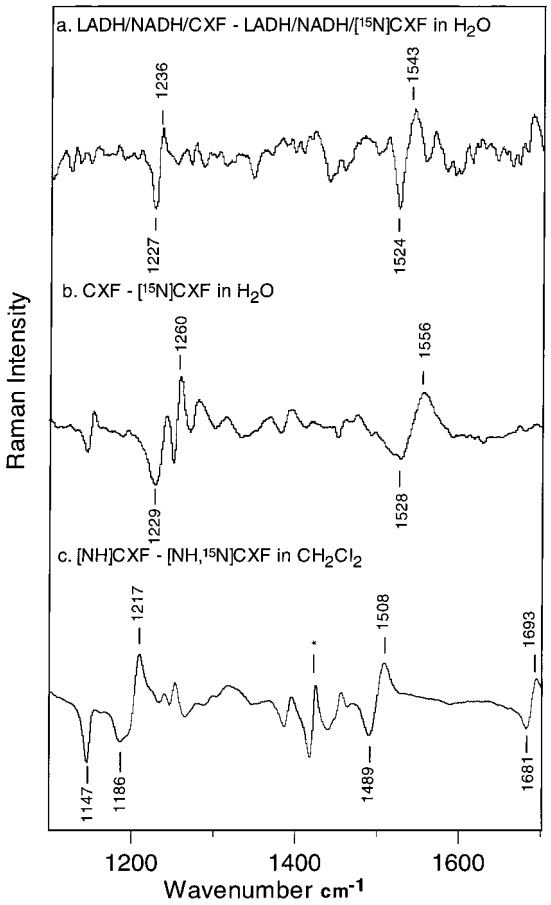

FIGURE 4: Raman difference spectra between unlabeled CXF and [^{15}N]CXF. (a) Between LADH/NADH/*N*-cyclohexylformamide (CXF) and LADH/NADH/[^{15}N]CXF at 4 °C in 100 mM pyrophosphate buffer at pH 9.6 in H_2O. The Raman bands labeled with an asterisk are due to bound NADH. (b) Between CXF and [^{15}N]CXF at 4 °C in H_2O. (c) Between CXF and [^{15}N]CXF (protonated amide) at 4 °C in methylene chloride. The Raman band labeled with an asterisk is due to solvent.

Theoretical Calculations. Our analyses were conducted on the model CXF systems shown in Chart 1. The geometries of the model compounds are fully optimized at the HF/6-31G** level, and the frequency calculations are performed on the optimized geometries using the same basis set. It is well-known that such calculations consistently overestimate the stretching force constants by about 20% (hence, frequencies by about 10%) and even more for double bonds containing oxygen or nitrogen (*15*, *16*). More accurate frequencies can be obtained by a "scaling" procedure wherein the force constants of a similar group of bonds, such as C−C stretches, C═O stretches, or N−H bends, are multiplied by empirically determined scaling factors before the vibrational frequencies are calculated (*16*). Such a procedure is particularly useful when the scaling factors for different bond types are significantly different. Here, we are only interested in three vibrational modes: the C═O and C−N stretches and the N−H bend. The scaling factors for the C−N stretch and N−H bend should be similar since the calculated C−N

Chart 1

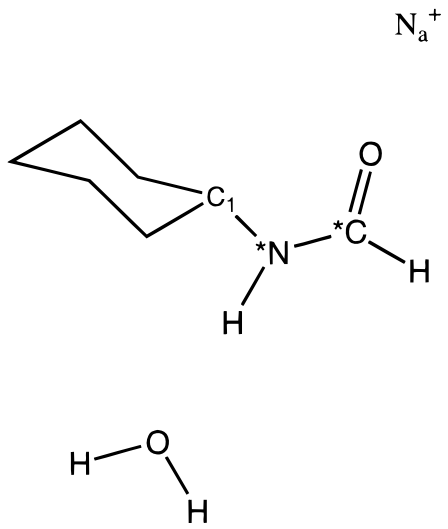

stretch and N−H bend frequencies are both overestimated by about 10%, while the C═O stretch mode is overestimated by about 15% (see below). On the basis of this observation, the coupling between C−N stretch and N−H bend should be reasonably well described in the calculated normal modes involving these two internal coordinates. The coupling between the C═O stretch and N−H bend internal coordinates may be somewhat underestimated in the calculations since the C═O stretch mode frequency is more overestimated than the N−H bend. However, such error is not serious enough to affect the assignments of these three modes as shown below. Therefore, we did not employ the nonuniform scaling procedure in these studies. Nevertheless, it is necessary to make a uniformly scaled correction when the calculated frequencies are compared to the experimental values.

Table 1 lists the experimentally observed values in aqueous solution, in methylene chloride, and in the LADH ternary complex. The calculated frequencies of the C═O and C−N stretches and the N−H(N−D) bend of the amide NH−CO moiety of isolated CXF, its complexes with water molecules, and/or a Na^+ ion in close contact with C═O (Chart 1) are shown in Table 2. The isolated CXF model is used to simulate the hydrophobic environment of methylene chloride. The Na^+−CXF model complex simulates the active site Zn^{2+} ion interacting with CXF in LADH. The monovalent ion takes into account, somewhat, the screening of some of the charge on Zn^{2+} that must take place at the LADH binding site since this ion is complexed with several protein groups. As pointed out above, the calculated frequencies of these three modes are higher than the experimentally observed values by about 10% for the C−N stretch and N−H(N−D) bend and by about 15% for the C═O stretch.

On the basis of the results of the normal mode calculations, the unusually large ^{13}C shift of the C═O stretch mode of CXF in H_2O can be explained. In isolated CXF, the C═O stretch frequency is calculated to be at 1966 cm^{-1} (Table 2), about 15% higher than the 1686 cm^{-1} band observed in methylene chloride (see Table 1). The calculated ^{13}C shift of this mode is 40 cm^{-1} (Table 2, after a 15% correction), which is very consistent with the observed ^{13}C shift in methylene chloride (41 cm^{-1}, Table 1). The calculations show that this normal mode also contains contributions from the C−N stretch; it can be described as an out-of-phase combination of the C═O and C−N stretch motions. Apparently, such coupling between the C═O and C−N internal coordinates is at least partially responsible for the larger-than-usual ^{13}C shift (should be about 37 cm^{-1} for a simple diatomic C═O stretch). The observed ^{13}C shift is even larger for CXF in aqueous solution (−46 cm^{-1}, Table 1). It is conceivable that in this case, its C═O bond is more polarized and its stretch force constant more reduced than those for CXF in methylene chloride. In this case, the coupling between C═O and C−N is likely enhanced which results in an even larger ^{13}C shift. However, our calculations did not accurately reproduce the ^{13}C shift observed in aqueous solution in any model because the ab initio method overestimates the C═O stretch force constant too much relative to the C−N stretch. Hence, the C═O stretch cannot be reduced enough to cause stronger coupling with the C−N stretch in any calculated model.

The calculations also provide a good description of the C−N stretch and N−H bend as judged by the agreement between calculated and observed shifts of these two modes upon isotopic substitution. According to the calculations, the internal N−H bending motion is coupled with the out-of-phase combination of the two C−N stretches of the C1−N−C moiety of CXF (see Chart 1) to form two modes at 1688 (the amide II mode) and 1308 cm^{-1} (the amide III mode) for the isolated molecule (listed as N−H bending and C−N stretch, respectively, in Table 2). Thus, the N−H bending mode observed in the experiment shows not only a moderate ^{15}N shift but also a small ^{13}C shift (Table 1). Upon deuterium exchange of the amide hydrogen, the coupling between the N−D bending and the out-of-phase C1−N−C stretch is removed. The N−D bending mode then shifts down to 1045 cm^{-1} in isolated CXF; the mode also contains a contribution from the C1−N stretch and has a small shift for ^{15}N (Table 2) but contains no contribution from the N−C stretch and has little isotope shift for ^{13}C═O, very consistent with experimental observations (Table 1). The out-of-phase C1−N−C stretch mode shifts to 1580 cm^{-1} (listed as the C−N stretch in Table 2) upon deuterium exchange in isolated CXF, about 100 cm^{-1} below the original N−H bending (or amide II) mode, which is also very consistent with the corresponding shift observed in the experiment (Table 1). A mode with N−H bending motion, coupled to several C−H bending motions of the ring, is predicted at 1276 cm^{-1}, which corresponds to the observed band at 1239 cm^{-1} in H_2O (Figure 1a). This mode shows no calculated ^{13}C═O shift and a 2 cm^{-1} ^{15}N shift, which is consistent with observations (Figure 1a). Upon deuterium exchange of N−H, the 1276 cm^{-1} mode is calculated to shift down to 1033 cm^{-1}, very close to the other mostly N−D bending mode at 1045 cm^{-1} (Table 2). In fact, two well-resolved bands about 10 cm^{-1} apart were observed in the Raman spectrum of [ND]CXF in methylene chloride near 950 cm^{-1} (data not shown), although only a broad band is observed for CXF in D_2O (Figure 2a). Finally, the observed frequency shifts of the C═O stretch, C−N stretch, and N−H bending modes induced by changing the solvent from methylene chloride to water have also been reasonably reproduced in the calculations. Compared to that of the isolated CXF, the C═O stretch mode in the CXF complexed with two water molecules shifts down by 31 cm^{-1} (15% correction) and the N−H bending mode shifts up by

Table 1: Observed Raman Bands of *N*-Cyclohexylformamide (CXF) under Various Conditions and Their Shifts in ^{13}C- or ^{15}N-Substituted Derivatives[a]

	water			methylene chloride			LADH/NADH/CXF		
mode	C═O stretch	C−N stretch	N−H(D) bend	C═O stretch	C−N stretch	N−H(D) bend	C═O stretch	C−N stretch	N−H(D) bend
native	1651	−	1552	1686	−	1507	−	−	1543
^{13}C	−46	−	−5	−41	−	−7	−	−	−
^{15}N	−2	−	−14	−2	−	−18	−	−	−9
ND	1649	1439	993	1681	1412	951	1633	1443	−
^{13}C,ND	−41	−17	−2	−41	−13	−2	−41	−12	−
^{15}N,ND	−3	−24	−4	−	−	−	−	−17	−

[a] The frequencies are in cm^{-1}. The numbers for the substituted molecules are frequency shifts relative to that of the unsubstituted molecule. The numbers for the ^{13}C,ND and ^{15}N,ND substituted molecules are frequency shifts relative to that of the ND-substituted molecule.

Table 2: Calculated Frequencies of Six *N*-Cyclohexylformamide (CXF) Model Systems[a]

	isolated CXF			CXF complexed with water near N−H			CXF complexed with water near C═O		
mode	C═O stretch	C−N stretch	N−H(D) bend	C═O stretch	C−N stretch	N−H(D) bend	C═O stretch	C−N stretch	N−H(D) bend
native	1966	1308	1688	1956	−1340	1723	1939	1330	1698
^{13}C	−47	−5	−6	−47	−8	−6	−47	−5	−7
^{15}N	−1	−6	−17	−1	−9	−17	−1	−5	−18
ND	1961	1580	1045	1950	1588	1072	1933	1589	1054
^{13}C,ND	−47	−8	−3	−47	−9	−2	−47	−9	−3
^{15}N,ND	−1	−9	−5	−1	−13	−2	−1	−11	−4

	CXF complexed with sodium near C═O			CXF complexed with water and sodium			CXF complexed with two waters		
mode	C═O stretch	C−N stretch	N−H(D) bend	C═O stretch	C−N stretch	N−H(D) bend	C═O stretch	C−N stretch	N−H(D) bend
native	1866	1362	1732	1859	1422	1764	1929	1354	1732
^{13}C	−46	−4	−8	−47	−5	−6	−47	−7	−7
^{15}N	−3	−5	−21	−4	−5	−16	−3	−8	−17
ND	1861	1617	1082	1855	1634	1120	1922	1596	1084
^{13}C,ND	−47	−10	−1	−41	−18	−1	−47	−10	−3
^{15}N,ND	−3	−17	−3	−4	−25	−1	−1	−15	−2

[a] Frequencies are given in cm^{-1} for the C═O stretch, the C−N, stretch and the N−H(N−D) bending: isolated CXF, one water hydrogen bonded to N−H, one water hydrogen bonded to C═O, a Na^+ coordinated with C═O, water hydrogen bonded to N−H and a Na^+ coordinated to C═O, and waters hydrogen bonded to both C═O and N−H. The numbers for the labeled molecules are the frequency shifts relative to that of the unlabeled molecule. The numbers for the ^{13}C,ND and ^{15}N,ND substitutions are frequency shifts relative to that of the ND-substituted molecule. All frequencies are obtained at the ab initio HF/6-31G** level on fully optimized geometries of the model complexes.

40 cm^{-1} (10% correction), consistent with the observed shifts of 35 and 45 cm^{-1}, respectively, when CXF is transferred from methylene chloride to aqueous solution (Tables 1 and 2). The calculated C−N stretch mode in deuterated CXF shifts up by 14 cm^{-1} (10% correction) when it is complexed with two water molecules (Table 2). This shift is fairly consistent with experiment; it is in the right direction but numerically smaller than the 25 cm^{-1} shift observed in the experiment (Table 1).

It is well established that the C═O stretch and the N−H bending frequencies are sensitive to the local hydrogen bonding and/or other electrostatic interactions; an increase of the hydrogen binding strength on the C═O bond will decrease the C═O stretch frequency, while an increase of the hydrogen binding strength on the N−H bond will increase the N−H bending frequency (*7*, *17*, *18*). However, little is known experimentally about if and how the change of the hydrogen bonding strength on the C═O bond will affect the N−H bending frequency, or vice versa, in an amide, since such experiments are extremely difficult (if even possible) to perform. Thus, vibrational normal mode calculations were performed on the CXF complexes with water hydrogen bonded to either N−H bond or C═O bond to study these effects.

Our results (Table 2) show that when the water is hydrogen bonded to the N−H bond, the N−H bending frequency shifts up by 35 cm^{-1} compared to that of the isolated CXF; at the same time, the C═O stretch frequency shifts down by 10 cm^{-1} and the C−N stretch frequency in the deuterated amide shifts up by 8 cm^{-1}. On the other hand, when water is hydrogen bonded to C═O, the C═O stretch frequency shifts down by 27 cm^{-1} while the N−H bend shifts up by 10 cm^{-1} and the C−N stretch in deuterated amide also shifts up by 10 cm^{-1}. Such results suggest that both C═O stretch and the N−H bending frequencies need to be obtained to determine hydrogen bonding interactions with either the C═O or the N−H moieties alone. Fortunately, according to the calculations, the shifts of the C═O stretch and the N−H bending frequencies induced by the hydrogen bond formation are additive. For example, the frequency shifts of the C═O stretch caused by formation of a hydrogen bond to the C═O bond are 27 cm^{-1} with a water molecule and 10 cm^{-1} with a N−H bond. The sum of the two shifts, 37 cm^{-1}, is identical to that caused by the formation of two simultaneous

hydrogen bonds to both moieties (Table 2). The same is true for the N−H bending frequency changes. The additive feature of the frequency shifts of the C═O stretch (or N−H bending) is not only true for normal hydrogen bonding but also true for much stronger electrostatic interactions. The calculations show that a Na^+ ion in close contact with the C═O bond of CXF and a hydrogen bond to the N−H moiety by a water molecule induces a -106 cm^{-1} shift in the C═O stretch frequency (Table 2), and this shift is almost the same as the sum of the C═O stretch shifts caused by a Na^+ ion near C═O alone (100 cm^{-1}) and by a water molecule near N−H alone (10 cm^{-1}). The same is true for the N−H bending frequency, where the upward shift caused by both water and Na^+ is 76 cm^{-1}, only 3 cm^{-1} different from the sum of the 35 cm^{-1} shift due to water alone and the 44 cm^{-1} shift due to Na^+ alone.

Thus, the observed frequency shift of the C═O stretch mode, $\Delta\nu_{C=O}$, can be treated as the sum of two terms: one due to the hydrogen bonding change on the local C═O bond, $\Delta\nu^{local}{}_{C=O}$, and the other due to the change near the remote N−H bond, $\Delta\nu^{remote}{}_{C=O}$. Similarly, the observed frequency shift of the N−H bending mode, $\Delta\nu_{N-H}$, can also be treated as the sum of the two terms $\Delta\nu^{local}{}_{N-H}$ and $\Delta\nu^{remote}{}_{N-H}$ due to the local change near the N−H bond and due to the remote change near the C═O bond, respectively. Additional calculations on models of CXF complexed with Na^+ or water fixed at various distances from the C═O or N−H bond suggest that for each 1 cm^{-1} shift of the C═O stretch frequency, the N−H bend frequency will shift about 0.4 cm^{-1} in the opposite direction if the environmental change is near the C═O bond ($\Delta\nu^{remote}{}_{N-H} = 0.4\Delta\nu^{local}{}_{C=O}$); for each 1 cm^{-1} shift of the N−H bending frequency, the C═O stretch frequency will shift about 0.3 cm^{-1} in the opposite direction if the environmental change is near the N−H bond ($\Delta\nu^{remote}{}_{C=O} = 0.3\Delta\nu^{local}{}_{N-H}$). Thus, we have

$$\Delta\nu_{C=O} = \Delta\nu^{local}{}_{C=O} - 0.3\Delta\nu^{local}{}_{N-H} \quad (1)$$

$$\Delta\nu_{N-H} = \Delta\nu^{local}{}_{N-H} - 0.4\Delta\nu^{local}{}_{C=O} \quad (2)$$

The variations in the numerical factors 0.3 and 0.4 obtained from different model calculations are ±0.05, which contributes an ∼20% error in the calculated $\Delta\nu^{local}{}_{C=O}$ and $\Delta\nu^{local}{}_{N-H}$ from the observed frequencies. Since the results of the calculations match the C═O stretch mode in deuterated amide better than in protonated amide due to the underestimation of the coupling between C═O stretch and N−H bending, the C═O stretch frequencies of the deuterated amides should be used in eqs 1 and 2 to calculate $\Delta\nu^{local}{}_{C=O}$ to reduce the error.

The Raman results show that the C═O stretch shifts by -16 cm^{-1} ($\Delta\nu_{C=O}$) and the N−H bending shifts by -9 cm^{-1} ($\Delta\nu_{N-H}$) in the LADH/NADH/CXF complex relative to their respective frequencies for CXF in aqueous solution, which yields a $\Delta\nu^{local}{}_{C=O}$ of -21 cm^{-1} and a $\Delta\nu^{local}{}_{N-H}$ of -18 cm^{-1}. Therefore, the local interaction with the C═O bond is stronger in the protein complex than that in aqueous solution, while that with the N−H bond is weaker. The C═O stretch shifts by -48 cm^{-1} ($\Delta\nu_{C=O}$) and the N−H bending shifts by 36 cm^{-1} ($\Delta\nu_{N-H}$) in the LADH/NADH/CXF complex relative to their respective frequencies for CXF in methylene chloride, which yields a $\Delta\nu^{local}{}_{C=O}$ of -43 cm^{-1} and a $\Delta\nu^{local}{}_{N-H}$ of 19 cm^{-1}. Therefore, the local interactions with both the C═O and N−H bonds are stronger in the protein complex than that in methylene chloride. By comparison of the frequencies of CXF in water relative to their respective frequencies for CXF in methylene chloride ($\Delta\nu_{C=O} = -32$ cm^{-1} and $\Delta\nu_{N-H} = 41$ cm^{-1}; Table 1), $\Delta\nu^{local}{}_{C=O} = -23$ cm^{-1} and $\Delta\nu^{local}{}_{N-H} = 32$ cm^{-1}. Our results indicate that the hydrogen bonding strength pattern for the C═O moiety is as follows: LADH/NADH/CXF complex > water > methylene chloride. On the other hand, the pattern for the N−H group is as follows: water > LADH/NADH/CXF complex > methylene chloride.

Estimate of Local Binding Enthalpies. Previous experimental studies have established that the C═O stretch frequency of a simple molecule is linearly correlated with the interaction enthalpy between a single electron acceptor and the C═O bond (*19*). Hence, shifts in frequency of this bond have been used to monitor the strengths of hydrogen bonds. For example, every 1 cm^{-1} shift of the C═O stretch frequency of acetone corresponds to a change of about 0.47 kcal/mol in hydrogen bond interaction enthalpy (*19*). However, for the C═O group in different molecules, the numerical values of the coefficient in the correlation differ because of varying C═O bond polarizabilities. Thus, it is necessary to determine the correlation for each molecule being studied to make accurate predictions. One method is to measure the hydrogen bond enthalpies ($-\Delta H$) between a C═O-containing molecule and a series of phenol derivatives, thereby constructing a $\Delta\Delta H$ versus frequency change correlation. However, this method cannot be applied to primary and secondary amides because both N−H and C═O will form hydrogen bonds with phenols.

Thus, an alternative method is used for CXF that employs the concept of (electron) "acceptor numbers" (AN) for various solvents (*20*). A linear relationship between the acceptor numbers of a series of solvents and vibrational frequencies of a given molecule in those solvents can often be found and is a measure of the polarizability of a given bond. The C═O stretch frequencies of acetone in a number of solvents have been measured, and they are plotted against the acceptor numbers of the solvents in Figure 5. It can be seen that the relationship between C═O frequencies and the acceptor numbers is indeed linear. A least-squares curve fitting of the data points yields $\Delta AN = -2.56\Delta\nu$ for acetone. The same procedure applied to CXF yields $\Delta AN = -0.99\Delta\nu$. However, a correction to the observed frequencies is necessary since the ab initio calculations suggest that only about 70% of C═O stretch frequency shift of CXF is due to the hydrogen bonding changes near the C═O bond while the rest is due to the hydrogen bond change near N−H (eq 1). After this correction, the relationship becomes $\Delta AN = -1.4\Delta\nu$. According to this relation, the C═O group of the amide is more polarizable than that of acetone, as expected. Since the correlation between the change in interaction enthalpy and the C═O frequency shift is known for acetone ($\Delta\Delta H_{acetone} = 0.47\Delta\nu$; enthalpy in kilocalories per mole and frequency in inverse centimeters), the acceptor number versus C═O frequency shift correlation for CXF can be converted to that between $\Delta\Delta H$ and $\Delta\nu$, using the conversion factor obtained from the two acetone correlations. The conversion yields $\Delta\Delta H_{CXF} = 0.26\Delta\nu$ for the CXF C═

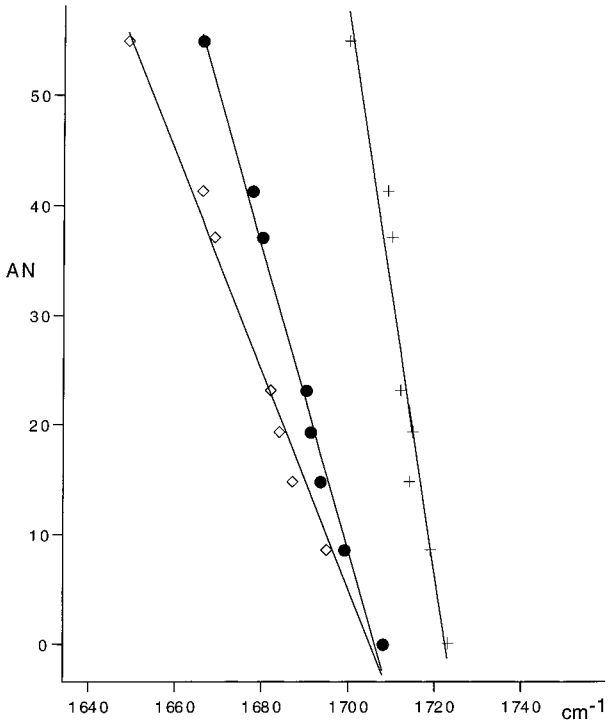

FIGURE 5: Effects of solvents on the C═O stretch frequency. Acetone (+), *N*-cyclohexylformamide (CXF) with deuterated N−D (◇), and that after 30% frequency reduction (●). The observed Raman frequencies of the C═O stretch are plotted against the "acceptor numbers" (AN) of the solvents. The solvents used in the Raman experiments were (in ascending order of the acceptor number, AN) hexane (0), CCl_4 (8.6), nitrobenzene (14.8), CH_3CN (19.3), $CHCl_3$ (23.1), CH_3CH_2OD (37.1), CH_3OD (41.3), and D_2O (54.8). The straight lines are the linear least-squares curve fits for the experimental data.

O stretch mode. The correlation coefficient of the relationship, 0.26, is very similar to that determined for *N*,*N*-dimethylpropionamide using the standard method (*19*), which is 0.24 (unpublished data).

Accordingly, the change in the effective local interaction energy between the C═O bond of the CXF and the enzyme resulting from a -21 cm^{-1} frequency shift (see above) is about 5.5 kcal/mol more stable in the LADH/NADH/CXF complex compared to that in aqueous solution. Although a direct quantitative relationship between the hydrogen bonding enthalpies and the O−H or N−H bending frequencies has not been firmly established, we have obtained an approximate correlation between the bending frequency shift and interaction energy change; every 10 cm^{-1} shift of the bending frequency corresponds to an ∼0.8−1.0 kcal/mol change in the energy (*21*). Thus, the -18 cm^{-1} shift of the N−H bending caused by the local interaction on the N−H bond corresponds to an ∼1.5 kcal/mol change in enthalpy in favor of the aqueous solution compared to that in the LADH ternary complex. On the basis of these observations, we conclude that the amide moiety of CXF contributes a net of about 4.0 kcal/mol of enthalpic energy stabilizing inhibitor binding to the protein.

Binding of CXF to LADH/NADH. Most of the Raman spectra were collected with the enzyme at pH 9.6, where high concentrations of soluble enzyme could be obtained. We determined the pH dependence of binding to assess the active form of the enzyme. Figure 6 shows that binding of CXF to the enzyme−NADH complex is independent of pH

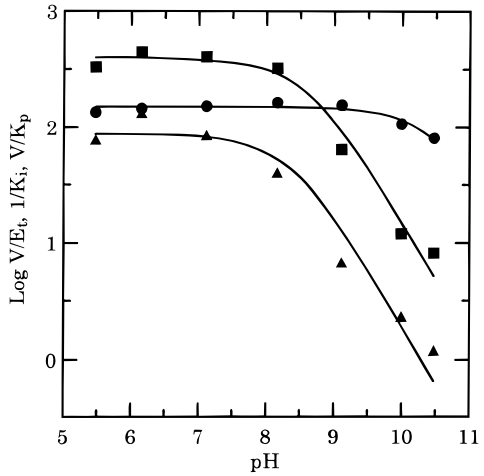

FIGURE 6: pH dependence of *N*-cyclohexylformamide binding. The dissociation constants for the formamide were determined from the competitive inhibition against varied concentrations of acetaldehyde. Buffers in the pH range of 5.5−9.0 contained 10 mM sodium pyrophosphate, sufficient phosphoric acid to obtain the desired pH, and sodium phosphate to make an ionic strength of 0.1. For pH values of 10.0 and 10.5, the 10 mM sodium pyrophosphate was adjusted to the desired pH and the ionic strength of 0.1 with sodium carbonate (*29*). Inhibition constants were determined at 25 °C with acetaldehyde as the varied substrate (0.22−2.0 mM at pH 5.5, 6, and 7, 0.11−1.0 mM at pH 8, and 0.056−0.50 mM at pH 9, 10, and 10.5) and NADH fixed at 0.2 mM. The concentration of inhibitor was varied over a 4-fold range. Initial velocities were determined using a Cary 118 spectrophotometer to measure the change in absorbance at 340 nm due to NADH oxidation. The calculation of turnover numbers was based on the concentration of enzyme active sites determined by titration with NAD^+ in the presence of 10 mM pyrazole, and the specific activity for titratable enzyme in the standard assay (*30*) was 2.7 units/mg. The inhibition data at each pH were fitted to the equation for competitive inhibition (*31*). The pH dependence for each kinetic parameter was fitted to the logarithmic form of the equation $Y = Y_{max}/(1 + K_b/[H^+])$ with the NONLIN program (C. M. Metzler, The Upjohn Co., Kalamazoo, MI): (■) V/K_m for acetaldehyde in units of mM^{-1} s^{-1}, where pK_b = 8.6 ± 0.1 and $(V/K_m)_{max}$ = 400 ± 64 mM^{-1} s^{-1}; (●) log(1/K_i) in units of mM^{-1}, where pK_b = 10.5 ± 0.1 and $(K_i)_{max}$ = 6.8 ± 0.2 μM; and (▲) V/E_t, turnover number in s^{-1}, where pK_b = 8.3 ± 0.2 and $(V/E_t)_{max}$ = 87 ± 24 s^{-1}.

below a p*K* of 10.5. The group in the E/NADH complex that is responsible for this p*K* may be a water bound to the catalytic zinc. In the three-dimensional structure of the ternary complex, the water is displaced by the oxygen of the amide, and it is presumed that the complex is electrostatically neutral (*1*). The enzyme is also maximally active at low pH. The binding of *N*-cyclohexylformamide is 1.6-fold tighter in D_2O than in H_2O, using 33 mM sodium phosphate buffer at pH 8. Addition of 0.2 M KCl did not significantly affect the binding of CXF.

DISCUSSION

N-Cyclohexylformamide is an analogue of the aldehyde substrates of LADH and binds to the enzyme/NADH complex in a manner that suggests that it could resemble the ground state structure of an active Michaelis complex (*1*). The oxygen binds to the catalytic zinc (2.3 Å) and forms a hydrogen bond to the hydroxyl group of Ser-48 (2.6 Å), and the carbonyl carbon is 4.0 Å from C4 of the nicotinamide ring in an orientation that would be suitable for direct transfer of a hydride ion to the *re* face of the carbonyl group (Figure 7).

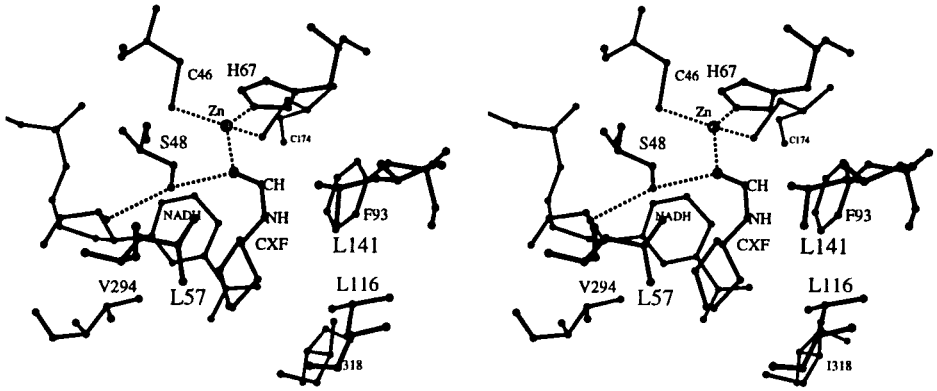

FIGURE 7: Binding of *N*-cyclohexylformamide to the LADH/NADH complex. The coordinates from PDB entry 1LDY were used (*1*).

How the enzyme activates the aldehyde for catalysis is the subject of this investigation. The C═O stretch mode of the amide of CXF when it is bound to the enzyme/NADH complex and the N−H bend have been measured. These results apply to protein in solution and represent native conditions. Changes in frequencies of these vibrational coordinates when the inhibitor binds relative to their values in water or in a hydrophobic environment describe the changes in local interactions that take place between the C═O and N−H bonds with their respective environments. The central result is that the C═O bond of the bound inhibitor has been polarized at the active site relative to its value in aqueous solution and even more so relative to that in a hydrophobic environment. The aldehyde bond is polarized by favorable, essentially electrostatic, interactions between the C═O moiety and the protein, presumably mostly due to the active site zinc with contribution from the hydrogen bond to the hydroxyl group of Ser-48. The total of these interactions is estimated in the Results to be equivalent to a hydrogen bond whose enthalpy is 5.5 kcal/mol stronger than it is for CXF in water or 11 kcal/mol stronger than that found in a hydrophobic (methylene chloride) environment.

Such evidence of C═O bond polarization is almost certainly important for the mechanism of catalysis in LADH. It is generally believed that the transition state for hydride transfer in the dehydrogenases contains considerable polar $^{+}C{=}O^{-}$ bond character. Hence, stabilization of such polar resonance structures would lower the height of the transition state barrier for hydride transfer. These results show directly that the effect of binding to the active site of LADH is to stabilize such structures as reported in the measurement of the ground state, Michaelis-like complex. It is not possible to estimate how much the transition state is lowered when CXF binds to LADH/NADH from this study. However, results from a similar system, lactate dehydrogenase, when a systematic series of measurements were taken on mutant proteins elucidated a correlation between ground state C═O bond polarization and changes in rate enhancement that suggested about half of this enzyme's catalytic power comes from such electrostatic stabilization (*22*).

The results also show that the number of conformations accessible to the inhibitor is decreased in the enzyme complex compared to water, hence demonstrating reactant immobilization. This conclusion comes about because the bandwidths of the vibrational modes are substantially narrowed upon complex formation (cf. Figure 3a). Vibrational bandwidths arise from a sum of homogeneous broadening (due to couplings to other internal modes of the molecule) and heterogeneous broadening. The latter is due to varying environments of the molecule which leads to a slightly different position of the central vibrational frequency (cf. ref *23* for a more complete discussion of this for the lactate dehydrogenase system). A reduced bandwidth is indicative of a reduced set of environments or reduced conformational accessibility. This also reduces the entropy of CXF when it is bound to LADH/NADH compared to that of CXF in solution. Since the entropy must be lost to bring the NADH and C═O bond of the aldehyde substrate together with the right orientation for the reaction to occur in LADH, the entropy loss realized in the ground state effectively lowers the transition state barrier and enhances the reaction rate (*24*).

The downward shift in the amide N−H bend of CXF when it binds to the enzyme/NADH complex from that in water is indicative of the loss of hydrogen bond interaction energy (a loss of about 1.5 kcal/mol as estimated in the Results). However, there is still apparent hydrogen bonding between the N−H moiety and the protein since the N−H bend frequency still lies at a higher frequency than that found in the hydrophobic non-hydrogen bonding environment of methylene chloride. In fact, it is estimated that there is an effective stabilizing interaction energy of the N−H group of bound CXF of about 1.5 kcal/mol relative to a hydrophobic environment. As a part of the crystallographic results of the LADH/NADH/CXF complex (*1*), there is no usual proton acceptor for the N−H moiety. However, the position of binding of the CXF to the enzyme/NADH complex suggested that the N−H of the amide could form a cation−π interaction (*25*) with the benzene ring of Phe-93 since the distance between the N and CE1 of Phe-93 is 3.0 Å (*1*). Complexation energies calculated for the *N*-methylformamide−benzene interaction at the HF/6-31G** level suggest that the interaction could contribute up to 2.5 kcal/mol to the binding, at the optimized distance of 3.7 Å (*26*). This is reasonably consistent with the value of 1.5 kcal/mol deduced from the changes in frequency of the N−H bend.

Finally, the measured inhibition constant of CXF in aqueous solution suggests that the total binding Gibbs free energy (G) on the CXF in the LADH/NADH/CXF complex is about 7 kcal/mol more favorable than that in aqueous solution. Since this made up of both enthalpic and entropic components, and the entropic $T\Delta S$ term of the Gibbs

free energy is almost certainly unfavorable, the binding enthalpy is greater than 7 kcal/mol. Our results show that a net of about 4 kcal/mol for the enthalpic binding energy is from the amide moiety and the rest apparently is from the hydrophobic interaction of the cyclohexyl ring with the protein residues. The binding of the carbonyl group to the catalytic zinc and the hydrogen bonding of the oxygen to the hydroxyl group of Ser-48 would account for about 5.5 kcal/mol of the enthalpic term. The binding of the amide N−H moiety is destabilizing. However, it clearly would be even more destabilizing if not for the cation−π interaction at the binding site.

ACKNOWLEDGMENT

We thank The University of Iowa Mass Spectroscopy Facility for the mass spectral determinations and the College of Medicine NMR Facility for use of the Varian 500 MHz NMR spectrometer.

APPENDIX

In this Appendix, the relative sizes of the Raman peaks from NADH and CXF are studied to help make the assignments of some of the Raman bands observed in Figure 3. Also, this section shows examples of the primary spectra used to generate the protein isotope-edited difference spectra presented in the text and the controls used to obtain them. In the difference Raman experiment, the LADH/NADH/CXF and LADH (or LADH/NADH/labeled CXF) samples were loaded into a split Raman cell and the Raman spectra were taken alternately from the two samples (*7*). Up to 10 runs were taken from each sample, and the spectra were then summed and averaged. The averaged spectrum so obtained for the LADH/NADH/CXF complex is shown in Figure 8a, while Figure 8b shows that of LADH. As a control experiment, the odd-numbered runs and even-numbered runs of the LADH sample were averaged, and their difference spectrum is shown in Figure 8c (enhanced by a factor of 20). This difference spectrum should be completely nullified; in fact, the noise in this spectrum, all of which is simple shot noise and is free from systematic subtraction artifacts, is 0.2% of the amide I band of LADH.

In the subtraction process, two Raman bands were used as internal references, the amide I band at 1660 cm^{-1} and the δCH band at 1450 cm^{-1}. A multiplication factor, typically ranging from 1.03 to 0.97, was applied to one of the spectra and adjusted so that these two bands were no longer visible in the final difference spectrum. Since the peak-to-peak intensity in the spectrum of the control (Figure 8c) is about 0.2% of the 1655 cm^{-1} band intensity of the original spectrum, the noise level in our other difference spectra is expected to be the same. Figure 8d shows the difference spectrum between LADH/NADH/CXF and LADH, with both the 1450 and 1660 cm^{-1} bands subtracted properly; Figure 8e shows the difference spectrum between LADH/NADH/^{13}C-labeled CXF and LADH. In these difference spectra, all the major peaks are from the dihydronicotinamide moiety of NADH in the ternary complex (cf. refs *27* and *28*). The intensity of the most prominent band at 1681 cm^{-1} is about 30% of the intensity of the major protein band at 1660 cm^{-1}. All other visible peaks in the difference

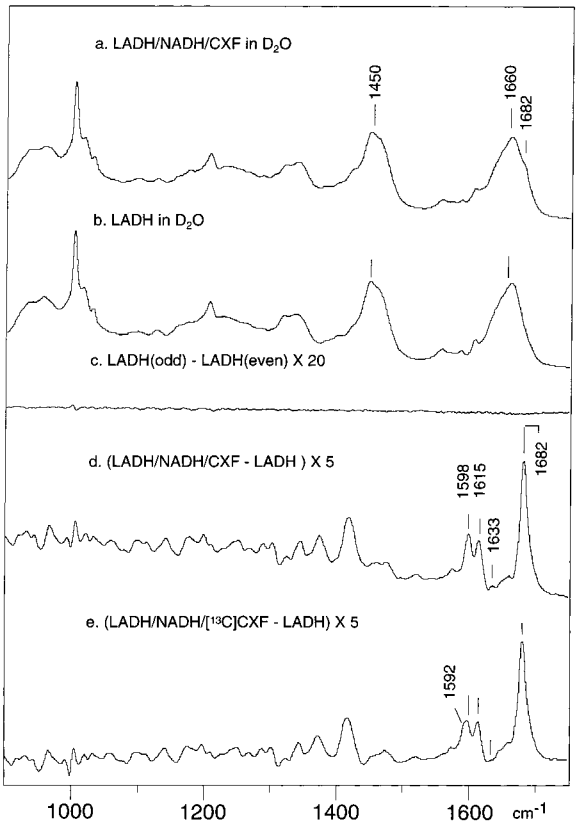

FIGURE 8: (a) Raman spectrum of LADH/NADH/*N*-cyclohexylformamide (CXF) at 4 °C in 100 mM pyrophosphate buffer at pH 9.6 (pH meter reading) in D_2O. (b) Raman spectrum of LADH at 4 °C in 100 mM pyrophosphate buffer at pH 9.6 (pH meter reading) in D_2O. (c) Difference spectrum between even-numbered LADH runs and odd-numbered LADH runs, with the result multiplied by a factor of 20. (d) Difference spectrum between spectra a and b, with the result multiplied by a factor of 5. (e) Raman difference spectrum between LADH/NADH/[^{13}C]CXF and LADH, with the result multiplied by a factor of 5.

spectra have intensities of about 1% of the 1660cm^{-1} protein peak or higher, well above the noise level. The Raman intensities of the CXF bands are very weak compared to those of the Raman bands of NADH. For example, the small peak at 1633 cm^{-1} in Figure 8d is the C═O stretch of CXF. This assignment is supported by its disappearance in ^{13}C-substituted CXF (Figure 8e) and the concomitant appearance of a shoulder to the 1598 cm^{-1} band at 1592 cm^{-1}, suggesting that the ^{13}C═O stretch lies at 1592 cm^{-1} in the labeled ternary complex. These peaks becomes more prominent in the isotope-edited spectrum shown in Figure 3a. Additional experiments suggested that the bound NADH bands at 1598 and 1615 cm^{-1} in Figure 8d are sensitive to CXF binding. Adjusting the relative CXF and NADH concentrations forming the LADH/NADH/CXF complex changed their intensities slightly. Since these NADH peaks are about 20 times more intense than the C═O stretch of CXF, a 5% difference in the concentration between CXF and its ^{13}C-labeled analogue is enough to introduce intensity changes of these bands comparable to the C═O stretch band intensity of the CXF in the isotope-edited difference spectrum. Thus, we believe a small imbalance between the CXF and ^{13}C-labeled CXF is responsible for the peaks labeled with an asterisk in the difference spectrum shown in Figure 3a.

REFERENCES

1. Ramaswamy, S., Scholze, M., and Plapp, B. V. (1997) *Biochemistry 36*, 3522−3527.
2. Plapp, B. V., Leidal, K. G., Smith, R. K., and Murch, B. P. (1984) *Arch. Biochem. Biophys. 230*, 30−38.
3. Delmas, C., de Saint Blanquat, G., Freudenreich, C., and Biellmann, J. F. (1983) *Alcohol.: Clin. Exp. Res. 7*, 264−270.
4. Schindler, J. F., Berst, K. B., and Plapp, B. V. (1998) *J. Med. Chem. 41*, 1696−1701.
5. Borch, R. F., Bernstein, M. D., and Durst, H. D. (1971) *J. Am. Chem. Soc. 93*, 2897−2904.
6. Risley, J. M., and Van Etten, R. L. (1980) *J. Am. Chem. Soc. 102*, 4609−4614.
7. Callender, R., and Deng, H. (1994) *Annu. Rev. Biophys. Biomol. Struct. 23*, 215−245.
8. Frisch, M. J., Trucks, G. W., Head-Gordon, M., Gill, P. M. W., Wong, M. W., Foresman, J. B., Johnson, B. G., Schlegel, H. B., Robb, M. A., Replogle, E. S., Gomperts, R., Andres, J. L., Raghavachari, K., Binkley, J. S., Gonzalez, C., Martin, R. L., Fox, D. J., Defrees, D. J., Baker, J., Stewart, J. J. P., and Pople, J. A. (1994) *Gaussian 94, Revision D*, Gaussian, Inc., Pittsburgh, PA.
9. Daimay, L.-V., Colthup, N. B., Fateley, W. G., and Grasselli, J. G. (1991) *The Handbook of Infrared and Raman Characteristic Frequencies of Organic Molecules*, Academic Press, San Diego, CA.
10. Colthup, N. B., Daly, L. H., and Wiberley, S. E. (1990) *Introduction to Infrared and Raman Spectroscopy*, 3rd ed., Academic Press, San Diego, CA.
11. Krimm, S. (1987) in *Biological Applications of Raman Spectroscopy: Raman Spectra and the Conformations of Biological Molecules* (Spiro, T., Ed.) pp 1−46, Wiley, New York.
12. Krimm, S., and Bandekar, J. (1986) *Adv. Protein Chem. 38*, 181−364.
13. Manor, D., Weng, G., Deng, H., Cosloy, S., Chen, C. X., Balogh-Nair, V., Delaria, K., Jurnak, F., and Callender, R. H. (1991) *Biochemistry 30*, 10914−10920.
14. Yue, K. T., Deng, H., and Callender, R. (1989) *J. Raman Spectrosc. 20*, 541−546.
15. Hehre, W. J., Radom, L., Schleyer, P. v. R., and Pople, J. A. (1986) *Ab-initio Molecular Orbital Theory*, Wiley, New York.
16. Pulay, P., Fogarasi, G., Pongor, G., Boggs, J. E., and Vargha, A. (1983) *J. Am. Chem. Soc. 105*, 7037.
17. Joesten, M., and Schaad, L. J. (1974) *Hydrogen Bonding*, Marcel Dekker, Inc., New York.
18. Vinogradov, S. N., and Linnel, R. H. (1971) *Hydrogen Bonding*, Van Nostrand Reinhold Co., New York.
19. Thijs, R., and Zeegers-Huyskens, T. (1984) *Spectrochim. Acta 40A*, 307−313.
20. Gutmann, V. (1978) *The Donor−Acceptor Approach to Molecular Interactions*, Plenum Press, New York.
21. Deng, H., Kurz, L., Rudolph, F., and Callender, R. (1998) *Biochemistry 37*, 4968−4976.
22. Deng, H., Zheng, J., Clarke, A., Holbrook, J. J., Callender, R., and Burgner, J. W. (1994) *Biochemistry 33*, 2297−2305.
23. Deng, H., Burgner, J., and Callender, R. (1992) *J. Am. Chem. Soc. 114*, 7997−8003.
24. Jencks, W. P. (1980) in *Molecular Biology, Biochemistry, and Biophysics* (Chapeville, F., and Haenni, A.-L., Eds.) pp 3−25, Springer-Verlag, New York.
25. Ma, J. C., and Dougherty, D. A. (1997) *Chem. Rev. 97*, 1303−1324.
26. Cho, H., and Plapp, B. V. (1998) *Biochemistry 37*, 4482−4489.
27. Chen, D., Yue, K. T., Martin, C., Rhee, K. W., Sloan, D., and Callender, R. (1987) *Biochemistry 26*, 4776−4784.
28. Yue, K. T., Martin, C. L., Chen, D., Nelson, P., Sloan, D. L., and Callender, R. (1986) *Biochemistry 25*, 4941−4947.
29. Gould, R. M., and Plapp, B. V. (1990) *Biochemistry 29*, 5463−5468.
30. Plapp, B. V. (1970) *J. Biol. Chem. 245*, 1727−1735.
31. Cleland, W. W. (1979) *Methods Enzymol. 63*, 103−138.

BI981477E